

RESEARCH PAPER

Glucagon-like peptide-1 receptor signalling reduces microvascular thrombosis, nitrosative and oxidative stress, systemic inflammation and platelet activation in endotoxaemic mice

Sebastian Steven^{1,2}, Kerstin Jurk², Maximilian Kopp¹, Swenja Kröller-Schön¹, Yuliya Mikhed¹, Kathrin Schwierczek², Siyer Roohani¹, Fatemeh Kashani¹, Matthias Oelze¹, Thomas Klein⁵, Sergey Tokalov², Sven Danckwardt^{2,3}, Susanne Strand⁴, Philip Wenzel^{1,2}, Thomas Münzel¹ and Andreas Daiber^{1,2}

From the Centre for Cardiology, Cardiology I¹; Centre for Thrombosis and Hemostasis²; Institute of Clinical Chemistry and Laboratory Medicine³; 1st Medical Clinic⁴, University Medical Centre of the Johannes Gutenberg-University, Mainz, Germany; Boehringer Ingelheim Pharma GmbH & Co. KG, Ingelheim, Germany⁵.

Running title: GLP-1 and microvascular thrombosis in endotoxaemia

Address correspondence to:

Prof. Dr. Andreas Daiber, Universitätsmedizin der Johannes Gutenberg-Universität Mainz, Zentrum für Kardiologie - Kardiologie I, Labor für Molekulare Kardiologie, Geb. 605 – Raum 3.262, Langenbeckstr. 1, 55131 Mainz, Germany, Phone +49 (0)6131 176280, Fax +49 (0)6131 176293, E-mail: daiber@uni-mainz.de

Keywords: endotoxaemia, DPP-4, GLP-1, oxidative stress, nitrosative stress, platelets, microvascular thrombosis

This article has been accepted for publication and undergone full peer review but has not been through the copyediting, typesetting, pagination and proofreading process which may lead to differences between this version and the Version of Record. Please cite this article as doi: 10.1111/bph.13549

Abstract

BACKGROUND AND PURPOSE

Excessive inflammation in sepsis causes microvascular thrombosis and thrombocytopenia associated with organ dysfunction and high mortality. The present studies aimed to investigate whether dipeptidyl peptidase-4 (DPP-4) inhibition and supplementation with glucagon-like peptide-1 (GLP-1) analogues improves endotoxaemia-associated microvascular thrombosis via immunomodulatory effects.

EXPERIMENTAL APPROACH

Endotoxaemia was induced in C57BL/6J mice by single injection of lipopolysaccharide (LPS) (17.5 for survival and 10 mg/kg for all other studies). For survival studies therapy was started 6 h after LPS injection. For all other studies drugs were administrated 48 h prior to LPS treatment.

KEY RESULTS

Endotoxaemic control mice showed severe thrombocytopenia, microvascular thrombosis in the pulmonary circulation (fluorescence imaging), increased lactate dehydrogenase (LDH)-activity, endothelial dysfunction and increased markers of inflammation in the aorta and whole blood (e.g. leukocyte-dependent oxidative burst, nitrosyl-iron haemoglobin (HbNO), a marker of nitrosative stress, and expression of inducible NO synthase). Treatment with linagliptin (DPP-4 inhibitor) and liraglutide (GLP-1 analogue) as well as genetic deficiency of DPP-4 (DPP4^{-/-} mice) improved all these parameters. In GLP-1 receptor deficient mice both drugs lost their beneficial effects and improvement of prognosis almost completely. Incubation of platelets and cultured monocytes (containing GLP-1r protein) with GLP-1 analogues inhibited the monocytic oxidative burst and platelet activation, in a GLP-1 receptor-dependent elevation of cAMP levels and protein kinase A (PKA) activation.

CONCLUSIONS AND IMPLICATIONS

GLP-1 receptor activation in platelets by linagliptin and liraglutide strongly attenuates endotoxaemia-induced microvascular thrombosis and mortality by a cAMP/PKA-dependent mechanism preventing systemic inflammation, vascular dysfunction and end organ damage.

Abbreviations

ACh	acetylcholine
cAMP	cyclic adenosine monophosphate
DIC	disseminated intravascular coagulation
DPP-4	dipeptidyl peptidase-4
ECL	enhanced chemiluminescence
ecSOD	extracellular superoxide dismutase
GLP-1	glucagon-like peptide-1
EPR	electron paramagnetic resonance spectroscopy
FB	fluorescent beads
HbNO	nitrosyl-haemoglobin
IL-6	interleukin-6
iNOS	inducible NO synthase (type 2)
L-012	8-amino-5-chloro-7-phenylpyrido[3,4-d]pyridazine-1,4-(2H,3H)dione sodium salt
LDH	lactate-dehydrogenase
LPS	lipopolysaccharide
NO	nitric oxide
Nox2	NADPH oxidase isoform 2
PGI ₂	prostacyclin
PKA	protein kinase A
PRP	platelet-rich plasma
qRT-PCR	quantitative reverse transcription polymerase chain reaction
ROS	reactive oxygen species
TF	tissue factor
VCAM-1	vascular adhesion molecule-1

TARGETS	
Other protein targets^a	Enzymes^d
<u>TNF-α</u>	<u>Adenylate cyclase</u>
GPCRs^b	<u>AMPK subfamily</u>
<u>GLP-1 receptor</u>	<u>phosphodiesterases</u>
Catalytic receptors^c	<u>PKA</u>
<u>TLR4</u>	

Ligands	
<u>acetylcholine</u>	<u>Insulin</u>
<u>cAMP</u>	<u>Linagliptin</u>
<u>Exenatide (exendin-4)</u>	<u>LPS</u>
<u>GLP-1</u>	<u>Liraglutide</u>
<u>ICAM-1</u>	<u>nitric oxide</u>
<u>IL-6</u>	<u>prostacyclin</u>
	<u>vascular cell adhesion protein 1</u>

These Tables of Links list key protein targets and ligands in this article that are hyperlinked* to corresponding entries in <http://www.guidetopharmacology.org>, the common portal for data from the IUPHAR/BPS Guide to PHARMACOLOGY (Pawson *et al.*, 2014), and are permanently archived in *The Concise Guide to PHARMACOLOGY 2015/16* (^{a,b,c,d}(Alexander *et al.*, 2015a; Alexander *et al.*, 2015b; Alexander *et al.*, 2015c; Alexander *et al.*, 2015d)).

Introduction

Glucagon-like peptide-1 (GLP-1) is an incretin hormone, which is released in response to food uptake (Wang *et al.*, 1995). Under physiological conditions, endogenous GLP-1 is rapidly degraded by dipeptidyl peptidase-4 (DPP-4). GLP-1 receptor (Bataille *et al.*, Last modified on 14/07/2015) signalling improves glucose metabolism via increased insulin release and reduced glucagon secretion of the pancreas in a cyclic adenosine monophosphate (cAMP)/protein kinase A (PKA)-dependent manner (Gromada *et al.*, 1997) but also exerts pleiotropic effects via other pathways (Pabreja *et al.*, 2014). GLP-1 analogue supplementation or DPP-4 inhibitor therapy is used to improve glycaemic control (Moritoh *et al.*, 2009; Sturis *et al.*, 2003), but also cardioprotective pleiotropic effects were observed in experimental studies (Apaijai *et al.*, 2013). There is also growing body of evidence for anti-inflammatory and anti-atherosclerotic effects by GLP-1 and DPP-4 inhibition (Matsubara *et al.*, 2012; Shah *et al.*, 2011). These anti-inflammatory effects were recently confirmed in a model of experimental sepsis (Kroller-Schon *et al.*, 2012; Ku *et al.*, 2010). Further, Gupta *et al.* demonstrated anti-aggregatory effects of the DPP-4 inhibitor sitagliptin on human platelets (Gupta *et al.*, 2012) without providing the mechanism underlying this phenomenon. In a recent publication, Cameron-Vendrig *et al.* provided evidence for platelet inhibition by the GLP-1 analog exenatide leading to reduced thrombus formation in an animal model (Cameron-Vendrig *et al.*, 2016). The authors also showed that the anti-aggregatory and antithrombotic effects of exenatide were associated with increased levels of cAMP.

Sepsis is a clinical syndrome characterized by and secondary to an overshooting immune response to an infection. Subsequent hypotension, coagulopathy and multiple organ dysfunction syndrome (MODS) are characteristic for septic shock. An average mortality of 40% makes it a leading cause of death in the Western societies (Levy *et al.*, 2012). Because of antibiotic resistance and an aging population, sepsis incidences raise and new therapeutic strategies are urgently needed.

The endotoxin lipopolysaccharide (LPS) from gram-negative bacteria triggers inflammation by binding directly via CD14 on monocytes and to endothelial cells via toll-like

receptors (TLR) after forming a complex with lipopolysaccharide binding protein (LBP) (Anas *et al.*, 2010). As a consequence, monocytes and vascular endothelial cells express tissue factor (TF) subsequently promoting thrombin and fibrin generation (Levi *et al.*, 1999; Schouten *et al.*, 2008). Under conditions of sepsis, massive thrombin generation leads to uncontrolled platelet activation, and finally to microvascular thrombosis, clotted capillaries and impaired perfusion of end organs. This clinical syndrome is known as disseminated intravascular coagulation (DIC) and includes both pro-coagulant thrombus formation and haemorrhage caused by consumption of clotting factors (Levi *et al.*, 2010).

Recently we demonstrated that DPP-4 inhibition by linagliptin as well as therapy with the GLP-1 analogue liraglutide improve survival in endotoxaemic rodents (Steven *et al.*, 2015a). However, the relevance of GLP-1 receptor signalling for beneficial effects of DPP-4 inhibition remains unclear. In the present study, we show that enhanced GLP-1 receptor signalling reduces microvascular thrombosis in a mouse model of endotoxaemia by inhibiting vascular inflammation and by direct cAMP/PKA-dependent inhibition of platelet aggregation. The importance of GLP-1 receptor signalling in mediating these phenomena was further substantiated by using GLP-1^{r-/-} knockout mice.

Methods

Materials

The Bradford reagent was obtained from BioRad (Munich, Germany). The DPP-4 inhibitor linagliptin was a kind gift from Boehringer Ingelheim Pharma GmbH & Co KG (Biberach an der Riss, Germany). Liraglutide was purchased as an injection pen (6 mg/ml in phenol-containing solution from Victoza/Novo Nordisk, Plainsboro, NJ). Exendin-4 was purchased from Abcam Biochemicals (Cambridge, MA, USA). For induction of endotoxaemia we used lipopolysaccharide (LPS) from *Salmonella typhosa* (#L6386 purified by phenol extraction, Sigma, St. Louise, MO, USA). Three batches of LPS were pooled and homogenized in a mortar, dissolved in NaCl and stocks were frozen at -80 °C. Upon thawing the stocks were

sonicated. L-012 (8-amino-5-chloro-7-phenylpyrido[3,4-d]pyridazine-1,4-(2H,3H)dione sodium salt) was purchased from Wako Pure Chemical Industries (Osaka, Japan). The Quanti Tect probe RT-PCR Kit was purchased from Qiagen (Hilden, Germany) and TaqMan probes from Applied Biosystems (Darmstadt, Germany). Fluorescent beads (Alignment Beads; 2.5 μ M) were obtained from Molecular Probes (Eugene, OR, USA). All other chemicals were of analytical grade and were obtained from Sigma-Aldrich, Fluka or Merck.

Animals and in vivo treatment

All animals were treated in accordance with the Guide for the Care and Use of Laboratory Animals as adopted by the US National Institutes of Health. Approval was granted by the Ethics Committee of the University Hospital Mainz and the Landesuntersuchungsamt Koblenz (#23 177-07/G 14-1-039). C57BL/6J, DPP-4^{-/-} and GLP-1 receptor^{-/-} (GLP-1r^{-/-}) mice were used. DPP-4^{-/-} mice were kindly provided by Dirk Reinhold (Otto-von-Guericke-University Magdeburg, Magdeburg, Germany) and generated by Didier Marguet (Centre d'Immunologie de Marseille-Luminy, Marseille, France) (Marguet *et al.*, 2000). GLP-1r^{-/-} mice were obtained from Charles River (Sulzfeld, Germany) and generated by Daniel Drucker (Mt. Sinai Hospital, Toronto, Canada) (Scrocchi *et al.*, 1996). Reduced DPP-4 activity in DPP-4^{-/-} mice was confirmed by DPP-4 activity measurement (**Supporting Information Fig. S1A**) and provided by Boehringer Ingelheim Pharma GmbH & Co KG (Biberach an der Riss, Germany). GLP-1r knock-out was verified by qRT-PCR (**Supporting Information Fig. S1B**). An endotoxaemia time-course for microvascular thrombus formation was established by using the fluorescence imaging methodology. Animals were divided into five groups and sacrificed under isoflurane anaesthesia at specific time points (0 h, 3 h, 6 h, 9 h, 12 h after LPS challenge (10 mg/kg)). For the main study, linagliptin (DPP-4 inhibitor; 5 mg/kg/day) or liraglutide (GLP-1 analogue; 200 μ g/kg/day) was administered 48 h before LPS challenge via osmotic minipumps (Alzet, Cupertino, CA, USA). For induction of endotoxaemia, LPS (10 mg/kg) from *Salmonella typhosa* was administered by single i.p. injections 24 h prior to the end of the experiment. Finally 72 h after start of therapy, mice were killed by exsanguination

in isoflurane anaesthesia, and the blood, aorta, lung and heart tissues were collected. Survival studies were performed by a single injection of LPS (17.5 mg/kg) in a lethal dose and drugs were administered 6 h after LPS treatment at the same concentration as defined above. Survival was monitored for 60 hours.

Quantification of nitrosyl-iron haemoglobin in whole blood by electron paramagnetic resonance spectroscopy (EPR)

EPR-based detection of Hb-NO was used to assess iNOS-derived NO production. Samples of venous blood for Hb-NO/EPR studies were obtained by puncture of the right heart of anesthetized mice and blood samples were immediately frozen/stored in liquid nitrogen as described before (Steven *et al.*, 2015a).

Cell Culture

All human excess material was obtained and handled in accordance with the Declaration of Helsinki and our institutional ethical guidelines. Human monocytes (MonoMac-1) (Ziegler-Heitbrock *et al.*, 1988) were grown in Dulbecco's modified Eagle's medium (Sigma) with 10 % fetal calf serum, 2 mmol/L L-glutamine, 1 mmol/L sodium pyruvate, 100 IU/mL penicillin, 100 µg/mL streptomycin, and 1x HAT (hypoxanthine, amethopterin/methotrexate, thymine). Experiments were performed in 96-well plates by adding linagliptin, liraglutide (1, 10, 100 µM) or solvent twice (24 and 4 hours) before the experiment. Furthermore, LPS (1 µg/ml; *S. typhosa*) was added 4 hours before experiment (all dilutions of liraglutide were made in buffer with phenol to exclude effects of the stabilizer). Finally, cells were used either for detection of oxidative burst by chemiluminescence or isolation of mRNA.

Chemiluminescence-based detection of oxidative burst of monocytes

Oxidative burst mainly reflects NADPH oxidase (Nox) and myeloperoxidase activity and was therefore used as a read-out for the degree of activation of cultured monocytes (Daiber *et al.*, 2004a). To measure whole monocyte ROS formation, cultured cells were stimulated with

the fungal endotoxin zymosan A (50 µg/ml) and assessed in PBS containing Ca²⁺/Mg²⁺ (1 mM) with L-012 (100 µM)-enhanced chemiluminescence (ECL) (Kroller-Schon *et al.*, 2014).

Reverse transcription real-time PCR (qRT-PCR)

mRNA expression was analysed with quantitative real-time RT-PCR as previously described (Hausding *et al.*, 2013). Briefly, total RNA from mouse aorta or MonoMac-1 cells was isolated (RNeasy Fibrous Tissue Mini Kit; Qiagen, Hilden, Germany), and 50 ng of total RNA was used for real-time RT-PCR analysis with the QuantiTect Probe RT-PCR kit (Qiagen). TaqMan[®] Gene Expression assays for iNOS, VCAM-1, IL-6, P-selectin and Nox2 as well as TBP were purchased as probe-and-primer sets (Applied Biosystems, Foster City, CA). The comparative Ct method was used for relative mRNA quantification. Gene expression was normalized to the endogenous control, TATA box binding protein (TBP) mRNA, and the amount of target gene mRNA expression in each sample was expressed relative to that of control.

Platelet count, fluorescence imaging of pulmonary microvascular thrombosis and LDH activity

Pulmonary microvascular thrombus formation was quantified by fluorescence imaging (IVIS Spectrum, PerkinElmer, MA, USA) using fluorescent beads (FB) (2.5 µM), according to Tokalov *et al.* (Tokalov *et al.*, 2012). FB were diluted in sterile sodium chloride solution (2x10⁵ beads/µl; 50 µl per animal) and injected into the tail vein of the animals (three hours after LPS injection). Lungs were removed from the animals and fluorescence was detected (excitation: λ640 nm emission: λ680 nm). Increased fluorescence signal was assumed as occlusion of microvessels (FB caught in embolic vessels). An automated haematology analyser (Sysmex KX-21N) was used to determine the number of thrombocytes in whole blood. Lactate dehydrogenase activity was analysed as a parameter for organ damage in the Department for Clinical Chemistry, University Medical Centre (Mainz, Germany), using the daily routine facilities for in-patient care (Iba *et al.*, 2009).

Immunohistochemistry and fluorescence microscopy

For immunohistochemistry lung segments were fixed in paraformaldehyde (4 %), paraffin-embedded and stained with primary antibodies against fibrinogen (abcam, UK); anti-rabbit biotinylated secondary antibodies were used at dilutions according to the manufacturer's instructions. For immunohistochemical detection ABC reagent (Vector, Burlingame, CA, USA) and then DAB reagent (peroxidase substrate Kit, Vector, Burlingame, CA, USA) as substrate were used. For fluorescence microscopy, lung segments were fixed as described above and nuclei were stained by 4',6-diamidin-2-phenylindol (DAPI). FB were visualized by excitation on their specific wave length (excitation: λ 640 nm emission: λ 680 nm).

Platelet isolation, incubation for Western blot, Dot blot and cAMP ELISA

Citrated whole blood was obtained from at least four different healthy volunteers by vein puncture, or taken from mouse by retro-orbital vein puncture using silanised glass capillaries. PRP was isolated by centrifugation (200 g for 10 min at 22 °C, slow deceleration). Murine or human platelets were incubated in PRP for 15 min with exendin-4 (abcam, UK), PGI₂ (0.2ng/ml), PKA inhibitor (1 μ M) (Sigma-Aldrich, USA) or solvent at 37 °C. Then, platelets were collected by centrifugation (700 g for 10 min at 22 °C), supernatant was removed and platelet pellet was resuspended in lysis buffer. Platelet protein was isolated for dot blot and Western blot analysis. For cAMP ELISA 1 M HCl solution was added to PRP and ELISA was performed according to the manufactures instructions (Cayman, USA).

Western blot and Dot blot analysis on murine and human platelets

Platelet proteins of mice and humans were separated by SDS-PAGE and blotted on nitrocellulose membrane as described before (Daiber *et al.*, 2004b). A monoclonal anti-pVASP^{Ser157} antibody (1:100, Calbiochem, UK) was used to detect cAMP-dependent phosphorylation, a monoclonal anti-GAPDH (1:1.000, GeneTex, USA) or anti- α -actinin (1:1000, Sigma-Aldrich, USA) antibody served as loading control (Schafer *et al.*, 2003). GLP-1 receptor protein was detected by a polyclonal anti-GLP-1 receptor antibody (1:1.000,

NOVUS, CO, USA). Detection and quantification were performed by ECL with peroxidase conjugated anti-mouse (1:10.000, Vector Lab., Burlingame, CA) secondary antibodies. Densitometric quantification of antibody-specific bands was performed with a ChemiLux Imager (CsX-1400M, Intas, Göttingen, Germany) and Gel-Pro Analyser software (Media Cybernetics, Bethesda, MD). Phosphorylation of PKA substrate protein was assessed by dot blot analysis of platelet protein homogenates, which were transferred to a Protran BA85 (0.45 µm) nitrocellulose membrane (Schleicher & Schuell, Dassel, Germany) by a Minifold I vacuum dot blot system (Schleicher&Schuell, Dassel, Germany). Each slot was washed with 250 µl PBS and the membrane was dried for 45 min at 60 °C. For detection of phosphorylated PKA substrate, a phospho^{Ser/Thr} PKA substrate antibody (Cell Signaling, USA) was used at a dilution of 1:1.000. Positive dots were detected by enhanced chemiluminescence after incubation with a peroxidase-coupled secondary antibody (1:10.000, Vector Lab., Burlingame, CA). All incubation and washing steps were performed according to the manufacturer's instructions. Densitometric quantification of the dots was performed as described in the Western blot section.

Measurement of thrombin generation and aggregation in murine and human platelet-rich plasma

Platelet-rich plasma (PRP) was prepared by centrifugation of citrate-anti-coagulated whole blood (mouse: 100 g for 4 min at 22 °C, slow deceleration, human: 200g for 10 min at 22 °C, slow deceleration), taken from mice by retro-orbital vein puncture using silanised glass capillaries or by vein puncture from healthy human volunteers. Human platelets were incubated for 15 minutes with exendin-4, liraglutide or solvent (all dilutions of liraglutide were made in buffer with phenol to exclude effects of the stabilizer). Platelet-dependent thrombin generation triggered by tissue factor or thrombin was assessed in PRP by fluorogenic-calibrated automated thrombography in vitro (Jurk *et al.*, 2011; Tchaikovski *et al.*, 2007). Thrombin- (2.5 U/ml in mouse, 0.2 U/ml in human) and ADP-induced (6 µM in mouse, 1 µM in human) aggregation was measured in diluted PRP supplemented with MgCl₂ (1 mM) and

CaCl₂ (2 mM) using light-transmission aggregometry (APACT, DiaSys, Germany). Gly-Pro-Arg-Pro (GPRP; 5 mM) was added to avoid clot formation (only in mouse PRP).

Isometric tension recordings

Perivascular fat was removed from every aorta, which were then cut into 4-mm segments. Rings were mounted on force transducers in organ bath chambers, pre-constricted with prostaglandin F_{2α} and concentration-relaxation curves in response to increasing concentrations of acetylcholine (ACh) were performed as described (Oelze *et al.*, 2006).

Statistical analysis

Results are expressed as mean ± SEM. Linear regression for correlation of thrombocytopenia and fluorescence was performed using Pearson correlation coefficient. Two-way ANOVA (with Bonferroni's correction for comparison of multiple means) was used for comparisons of vasodilator potency and efficacy in response to the endothelium dependent vasodilator acetylcholine (ACh). One-way ANOVA (with Bonferroni's correction for comparison of multiple means) was used for comparisons of fluorescence imaging, platelet count, LDH, mRNA expression, HbNO-levels, oxidative burst, CAT, cAMP-levels, Western blot and dot blot results. Maximal aggregation and inclination were analysed by using t-test. p values < 0.05 were considered as statistically significant. All statistical analyses were performed using GraphPad Prism 6.0d.

Results

DPP-4 inhibition and GLP-1 analogue therapy reduce myelomonocytic, iNOS-dependent NO-formation and monocyte-derived oxidative stress

LPS-challenge induced a strong increase in iNOS-derived NO formation in whole blood of wild-type animals, which was significantly reduced by linagliptin and liraglutide therapy. A comparable effect was found in endotoxaemic DPP-4^{-/-} mice (**Figure 1A**) but not in response

to therapy with the GLP-1 analogue in endotoxaemic GLP-1^{r/-} mice (**Figure 1B**). Suppression of iNOS activity by DPP-4 inhibitor therapy in GLP-1^{r/-} mice was only marginal (**Figure 1B**). In accordance, iNOS expression in aortic tissue was strongly increased in endotoxaemic wild-type mice, probably by infiltrated immune cells, and reduced by linagliptin and liraglutide treatment (**Supporting Information Fig. S2A**). In previous studies the read-out for iNOS activity (HbNO) was strictly correlated with hypotension in the endotoxaemic mice (Steven *et al.*, 2015a).

Next we examined direct effects of DPP-4 inhibition and GLP-1 analogue on cultured human monocytes (MonoMac-1) in response to 4 h LPS incubation. Incubation of monocytes with linagliptin or liraglutide dose-dependently reduced zymosan A-induced formation of reactive oxygen species (ROS) generation (**Figure 1C**). Also in freshly isolated monocytes from human whole blood, ex vivo incubation with another GLP-1 analogue, exendin-4, reduced the intensity of the oxidative burst (**Figure 1D**). Likewise, the mRNA expression of the NADPH-oxidase subunit Nox2 was strongly stimulated by LPS treatment (**Figure 1E**) and significantly inhibited by incubation of the cells with linagliptin and liraglutide in a dose-dependent manner. These data are in accordance with our previous observations that in vivo linagliptin and liraglutide therapy prevent oxidative burst in whole blood from LPS-treated rats (Steven *et al.*, 2015a). In addition, several DPP-4 inhibitors suppressed the activation of monocytes and neutrophils, their adhesion to cultured endothelial cells and infiltration of leukocytes to the vascular wall of LPS-treated rats (Kroller-Schon *et al.*, 2012).

Effects of DPP-4 inhibition and GLP-1 analogue therapy on endotoxaemia-induced thrombocytopenia and pulmonary microvascular thrombosis

LPS-induced endotoxaemia led within 12h to a severe drop of platelet count and an increase in pulmonary microvascular thrombus formation over time, which was negatively correlated to time after LPS injection ($r=-0.8923$; $p=0.0209$) (**Figure 2A**).

DPP-4-inhibition by linagliptin and supplementation with the glucagon-like peptide-1 (GLP-1) analogue liraglutide or genetic knockout of DPP-4 (DPP-4^{-/-}) prevented the fall in

thrombocyte numbers significantly. In endotoxaemic GLP-1 receptor knockout mice (GLP-1^{-/-}) linagliptin and liraglutide therapy had no protective effect (**Figure 2B**). The activity of lactate dehydrogenase (LDH), determined as a parameter of end organ damage due to microvascular thrombosis and tissue hypoxia was markedly increased in septic animals and significantly reduced by linagliptin and liraglutide therapy (**Figure 2C**). Linagliptin and liraglutide therapy as well as DPP-4 deficiency largely prevented LPS-induced microvascular thrombus formation in lungs (**Figure 3A**). In contrast, linagliptin or liraglutide failed to improve pulmonary microvascular thrombosis in GLP-1^{-/-} mice, pointing towards an important role of GLP-1 receptor signalling in this phenomenon (**Figure 3A**).

Fluorescent beads (FB) injected for imaging of microvascular thrombosis were also detected by fluorescence microscopy of pulmonary sections. In pulmonary sections of endotoxaemic wild-type mice clusters of FB were detectable, whereas in lungs of linagliptin and liraglutide treated and LPS-challenged animals we detected almost no fluorescent cluster formation in pulmonary vessels. A similar protective effect was established in DPP-4^{-/-} mice. Interestingly, in animals lacking the GLP-1 receptor, linagliptin and liraglutide therapy had no protective effect (**Figure 3B**). Fibrinogen staining co-localized with the fluorescence signal of FB, indicating that FB cluster formation was correlated to LPS induced microthrombi formation (**Figure 3C**).

DPP-4 inhibition and GLP-1 analogue therapy reduce platelet reactivity via GLP-1 receptor/cAMP/PKA dependent pathway in mice and human

Western blot analysis revealed substantial GLP-1 receptor protein expression in isolated murine platelets (**Figure 4A**). Furthermore, GLP-1 receptor protein was detectable in human monocytes and in higher concentrations in human platelets (**Figure 4B**). In platelet-rich plasma (PRP) of linagliptin and liraglutide treated animals, thrombin generation (endogenous thrombin potential (ETP)) triggered by tissue factor (TF) was significantly reduced (**Figure 4C**). In contrast, thrombin generation of GLP-1r deficient platelets was significantly increased compared to control and DPP-4^{-/-} mice (**Figure 4D**). Additionally, platelet aggregation of

GLP-1^{r/-} mice was significantly increased in response to thrombin and ADP compared to wild-type animals (**Figure 4E**). Incubation of murine platelets with the GLP-1 analogue exendin-4 induced a robust increase of VASP^{Ser157} phosphorylation, a read-out for increased intracellular cAMP formation (**Figure 4F**). In isolated platelets of GLP-1^{r/-} mice, in vitro incubation with exendin-4 showed no increase of VASP phosphorylation at Ser¹⁵⁷ (**Figure 4G**). These results are compatible with an inhibitory effect of GLP-1 analogue on platelet aggregation, which is mediated, at least in part, via the cAMP/PKA pathway.

In vitro experiments on human platelets revealed a dose-dependent, inhibitory effect of the GLP-1 analogue liraglutide and exendin-4 on platelet activity. Both analogues reduced maximal platelet aggregation in response to ADP (**Figure 5A**) and thrombin (**Supporting Information Fig. S3A-B**). Thrombin generation of human platelets in PRP in response to thrombin (peak of thrombin generation and ETP) was significantly reduced by GLP-1 (**Figure 5B/C, Supporting Information Fig. S3C-D**). Next, PRP from different healthy volunteers was isolated and incubated with increasing concentrations of the GLP-1 analogue exendin-4. Levels of cAMP, measured by ELISA, increased dose-dependently in response to GLP-1 (**Figure 5D**). We also observed a dose dependent increase of PKA-dependent phosphorylation of VASP^{Ser157} and phosphorylation of PKA substrate (Ser/Thr) in response to the GLP-1 analogue exendin-4 (**Figure 5E and 5G**). Exendin-4 induced phosphorylation of VASP^{Ser157} was inhibited by the PKA-Inhibitor (6-22 amide) reflecting the important role of PKA for GLP-1 effects on platelets (**Figure 5F**).

DPP-4 inhibition and GLP-1 analogue therapy prevent LPS-induced endothelial dysfunction and vascular inflammation and improve survival of endotoxaemic mice

In a last set of experiments we also confirmed our previous findings on pharmacological DPP-4 inhibitor and GLP-1 supplementation therapy in rats and mice (Kroller-Schon *et al.*, 2012; Steven *et al.*, 2015a), but this time by using a genetic approach, DPP-4 knockout and GLP-1^{r/-} mice. Recently, we reported on improved survival of endotoxaemic wild type mice

under linagliptin and liraglutide treatment (Steven *et al.*, 2015a). As expected for a GLP-1 analogue, treatment of GLP-1r^{-/-} with liraglutide 6 h post LPS injection did not improve survival of endotoxaemic mice and untreated GLP-1r^{-/-} even showed aggravated mortality in response to LPS challenges (**Figure 6**). However, DPP-4 inhibition by linagliptin significantly reduced mortality in GLP-1r^{-/-} mice underlining the previously suggested GLP-1r-independent effects of DPP-4 inhibitors due the plethora of targets of DPP-4 (Steven *et al.*, 2015a; Steven *et al.*, 2015b). LPS treatment induced endothelial dysfunction as indicated by a reduced ACh-induced vasodilation, all of which was markedly improved by treatment with linagliptin, liraglutide and, as a new result, by DPP-4 knockout (**Supporting Information Fig. S4A-B**). To differentiate, whether the protective effect of DPP-4 inhibition relates to an increase of GLP-1 levels and stimulation of down-stream GLP-1 receptor signalling or other mechanisms, linagliptin and liraglutide therapy was applied in endotoxaemic GLP-1r^{-/-} mice. These studies revealed that linagliptin and liraglutide protective effects were almost lost in the absence of the GLP-1r as compared to wild-type animals (**Supporting Information Fig. S4C**). As shown before^{11, 25}, LPS treatment increased aortic mRNA expression of P-selectin, VCAM-1 and IL-6 compared to control and linagliptin or liraglutide therapy reduced expression of these genes significantly (**Supporting Information Fig. S2B-D**).

Discussion

With the present studies, we describe a hitherto unknown mechanism of platelet inhibition by GLP-1, namely a receptor/cAMP/PKA signalling pathway with potential important clinical implications for the treatment of septic shock. Both, DPP-4 inhibition and treatment with GLP-1 analogues were able to attenuate thrombin generation in platelet-rich plasma. In vivo, these interventions prevented endotoxaemia-induced endothelial dysfunction and also prevented disseminated intravascular coagulation and microvascular thrombus formation.

Previous studies have demonstrated that DPP-4 inhibitors such as linagliptin exhibit pleiotropic vasodilatory, antioxidant, and anti-inflammatory properties that were clearly independent of its glucose-lowering properties (Kroller-Schon *et al.*, 2012). In animals with

LPS-induced septic shock, linagliptin improved endothelial dysfunction and ameliorated vascular superoxide formation. Furthermore expression of NADPH oxidase subunits and white blood cell infiltration into the vasculature were reduced. Importantly, linagliptin was very effective in inhibiting oxidative burst in isolated activated human neutrophils and it suppressed their adhesion to activated endothelial cells (Kroller-Schon *et al.*, 2012).

These findings were extended by the demonstration that linagliptin therapy and DPP-4 knockout was able to improve survival of endotoxaemic mice. Likewise, we established that DPP-4 inhibition reduced iNOS dependent NO production and aortic expression of iNOS, ICAM-1, MCP-1, TNF- α , VCAM-1 and IL-6 and simultaneously improved vascular function. The beneficial effects were attenuated in AMP activated kinase (alpha1) knockout animals suggesting that part of these beneficial effects were mediated by the AMPK (Steven *et al.*, 2015a). In addition, bleeding time was ameliorated by DPP-4 inhibition and GLP-1 supplementation in septic rats, as a first evidence for a role of DPP-4/GLP-1 signalling in haemostasis, however, without providing any mechanistic explanation. Interestingly, all these beneficial effects seem to be independent of blood glucose lowering effects of the antidiabetic drugs since we found no changes in blood glucose levels. Neither in linagliptin treated (Kroller-Schon *et al.*, 2012), nor in DPP4^{-/-} or GLP-1r^{-/-} animals blood glucose levels or HbA1c were effected (not shown).

The present studies demonstrate leukocyte-derived NO formation in whole blood (HbNO) and the expression of iNOS to be increased in endotoxaemia and normalization by linagliptin and liraglutide therapy in septic mice. The lack of effect of both treatments on HbNO formation in GLP-1r^{-/-} points to a crucial role of the GLP-1r for modulation of iNOS-derived NO generation. These findings go along with findings of Chang *et al.*, who showed reduced iNOS protein expression in Raw264.7 macrophage cells after stimulation of the GLP-1r with the GLP-1r analogue exendin-4, which was mediated via the activation of cAMP/PKA pathway (Chang *et al.*, 2013). As shown previously, vascular function and inflammation (IL-6, VCAM-1, P-selectin) was significantly improved in LPS-treated animals by DPP-4 inhibition and by treatment with the GLP-1 analogue. The previously shown

beneficial effect on mortality (Steven *et al.*, 2015a) was absent in GLP-1^{-/-} treated with liraglutide, nevertheless linagliptin improved survival significantly compared to untreated wild-type and GLP-1^{-/-} mice (**Figure 6**). This points towards GLP-1 independent immunomodulatory effects of DPP-4 inhibition. DPP-4 was also described as an adenosine deaminase (ADA)-binding protein and to regulate the subcellular localization and activity of this enzyme, which has known immunomodulatory functions (Kameoka *et al.*, 1993; Martin *et al.*, 1995). Several other protein targets were described for DPP-4 such as caveolin-1, kidney Na⁺/H⁺ ion exchanger 3, thromboxane A₂ receptor, CXCR4, CXCL12 (SDF-1), fibronectin and many more (Zhong *et al.*, 2013), most of them being involved in the regulation of inflammation and coagulation.

Linagliptin and liraglutide also dose-dependently inhibited the mRNA expression of the ROS generating enzyme NADPH oxidase isoform 2 (Nox2) and generation of reactive oxygen species (ROS) in cultured monocytes (MonoMac-1 cells) and the latter parameter also in freshly isolated human monocytes. Recently Arakawa *et al.* and Matsubara *et al.* demonstrated anti-atherosclerotic and anti-inflammatory effects of GLP-1 in mice, which contribute to the inhibition of NFκB/p65 nuclear translocation by increased cAMP levels in macrophages (Arakawa *et al.*, 2010; Matsubara *et al.*, 2012). Furthermore, Dai *et al.* suggest that GLP-1 inhibits ox-LDL uptake through PKA/CD36 pathway in macrophages (Dai *et al.*, 2014). Prostacyclin (PGI₂) and the stable analogue iloprost are known to increase intracellular cAMP and to reduce oxidative burst in canine monocytes (Gryglewski *et al.*, 1987; Simpson *et al.*, 1987).

As expected in GLP-1^{-/-} mice, the GLP-1 analogue liraglutide showed no protective effect on endothelial (vascular) function suggesting that the beneficial effects of liraglutide in endotoxaemia are mainly mediated by GLP-1 receptor signalling.

A hallmark of septic shock, also determining to a large extent survival in these animals, is disseminated intravascular coagulation (DIC). DIC is a pathological process characterized by the widespread activation of the clotting cascade that results in the formation of blood clots in small blood vessels throughout the body. This will compromise

tissue blood flow and will cause multiple end organ failure. In addition, since the coagulation process consumes clotting factors and platelets, normal clotting is disturbed and severe bleeding can occur at various sites. Previously we demonstrated that DPP4 inhibition improved haemostasis in septic animals (tail bleeding time and activated partial thromboplastin time) (Steven *et al.*, 2015a) but it remained to be established whether DIC might be also beneficially influenced by GLP-1 analogue therapy and by what mechanism.

To quantify microvascular thrombus formation as a consequence of DIC, we used in the present studies imaging with fluorescent beads (FB). More recently, Tokalov *et al.* employing this technique, established the distribution of FB in healthy hairless mice by demonstrating that 2.5 μm sized beads pass through the pulmonary circulation and accumulate in spleen or liver (Tokalov *et al.*, 2012). Our experiments revealed similar findings for lungs of non-endotoxaemic animals, whereas the fluorescence signal in lungs of mice challenged with LPS was markedly increased, which was improved by GLP-1 and DPP-4 inhibition (**Figure 3**). By using fluorescence microscopy we further detected FB in the pulmonary microcirculation and were able to co-localize them with fibrin deposits. Based on our time-course data obtained from endotoxaemic mice, platelet count and microvascular thrombosis are strongly correlated.

Next we tested whether murine or human platelets may contain a GLP-1r. Since the presence of the GLP-1 receptor on human platelets has not been evaluated at the time the study was performed, we isolated platelets from human and murine whole blood. GLP-1 receptor protein was identified by Western blot technique in human monocytes and in higher concentrations in murine and human platelets.

Importantly, inhibition of DPP-4 by linagliptin or GLP-1 analogue treatment by liraglutide strikingly reduced the drop of platelet count and normalized LDH activity as a marker for end organ damage. These data provide a potential explanation for our previous results on reduced mortality in endotoxaemia provided by linagliptin and liraglutide (Steven *et al.*, 2015a).

The DPP-4 inhibitor linagliptin contains a methylxanthine structure. These compounds inhibit phosphodiesterase (PDE) leading to increased intracellular cAMP levels e.g. in cultured human macrophages (Matsubara *et al.*, 2012). Since cAMP has been shown to have also potent anti-aggregatory effects in platelets, we hypothesized that increased cAMP formation and subsequent PKA activation may represent the anti-aggregatory mechanism (as with PGI₂) in response to DPP-4 inhibition.

Indeed, further experiments revealed that exposure of human and murine platelets to the GLP-1r agonist exendin-4 increase VASP phosphorylation at serine 157 (a readout of PKA activity), an effect that was wiped out in platelets from GLP-1r^{-/-} animals. Exendin-4 also increased platelet cAMP content and the phosphorylation of PKA substrate, all compatible with a GLP-1r mediated activation of the cAMP/PKA pathway. Liraglutide and exendin-4 were tested head-to-head in most ex vivo assays to show that this is a class effect of these drugs.

Thrombin generation in platelet-rich plasma of non-endotoxaemic liraglutide-treated animals was significantly reduced. Both GLP-1 analogues tested in this study, liraglutide and exendin-4, showed strong inhibitory effects on human platelet activation. Likewise, thrombin generation was markedly increased in GLP-1r^{-/-} mice. The high plasma protein binding affinity of liraglutide might be the reason, that higher concentrations of the drug were needed in PRP to induce similar effects as compared to exendin-4 (Plum *et al.*, 2013). Nevertheless, the here used concentrations for in vitro experiments are higher than usually observed for plasma levels in diabetic patients treated with clinical doses of linagliptin or liraglutide (Elbrond *et al.*, 2002; Graefe-Mody *et al.*, 2012). Therefore, higher drug doses might be required to observe effects on platelet function in patients. Taken together, these results clearly demonstrate, that GLP-1 receptor signalling via cAMP/PKA is a strong regulator of platelet activation, relevant for primary (aggregation) and secondary (thrombin formation) haemostasis, in mouse and human.

Very recently, Cameron-Vendrigs *et al.* demonstrated an inhibitory action of the GLP-1 analogue exenatide on platelet aggregation ex vivo and thrombus formation in animals

(Cameron-Vendrig *et al.*, 2016). In accordance to our data, they were able to detect the presence of the GLP-1 receptor on platelets. Furthermore, they were able to link these beneficial effects to elevated cAMP levels and observed a loss of platelet inhibition by exenatide in GLP-1^{-/-} mice (Cameron-Vendrig *et al.*, 2016). Thus, our data support the findings of Cameron-Vendrigs *et al.* and proof the effectiveness of GLP-1 to inhibit platelet activation via cAMP/PKA pathway in the setting of disseminated intravascular coagulation.

In conclusion, the present studies identified the existence of GLP-1r in platelets. GLP-1r signalling (cAMP/PKA pathway mediated) is demonstrated as a new and powerful therapeutic approach to improve vascular function and to reduce intravascular thrombus formation, DIC and survival in the setting of septic shock. The anti-inflammatory and anti-thrombotic action of GLP-1 may represent a novel approach to improve prognosis of septic patients. However, clinical trials are needed to further evaluate the use of GLP-1 analogues or DPP-4 inhibitors in this particular group of patients.

Acknowledgments

We are indebted to Angelica Karpi, Jörg Schreiner, Jessica Rudolph and Bettina Mros (Centre for Cardiology, University Medical Centre, Mainz, Germany) for expert technical assistance. Sebastian Steven holds a Virchow-Fellowship from the Centre of Thrombosis and Haemostasis (Mainz, Germany) funded by the Federal Ministry of Education and Research (BMBF 01EO1003). Andreas Daiber, Philip Wenzel, Kerstin Jurk, Kathrin Schwierczek and Sven Danckwardt were supported by the Federal Ministry of Education and Research (BMBF 01EO1003). Yuliya Mikhed holds a stipend from the International PhD Programme on the “Dynamics of Gene Regulation, Epigenetics and DNA Damage Response” from the Institute of Molecular Biology gGmbH, (Mainz, Germany) funded by the Boehringer Ingelheim Foundation. A part of the study was supported by a research grant from Boehringer Ingelheim Pharma GmbH & Co. KG, Ingelheim, Germany. This paper contains results that are part of the doctoral thesis of Maximilian Kopp.

Author contributions

S.Ste., A.D. designed and performed research, analysed data, and wrote the paper; M.K., S.K.-S., Y.M., K.S., S.R., F.K., M.O., S.T., S.Str. designed and performed research, and analysed data; K.J. designed research, analysed data, and critically revised the paper; T.K., S.D., P.W. analysed data, and critically revised the paper; T.M. wrote and critically revised the paper.

Conflict of interest

A.D. and T.M. received research grant support from the manufacturer of linagliptin, Boehringer Ingelheim Pharma GmbH & Co. KG, Ingelheim, Germany. T.K. is an employee of Boehringer Ingelheim Pharma GmbH & Co. KG, Ingelheim, Germany. All other authors have no competing financial interests.

References

Alexander SP, Davenport AP, Kelly E, Marrion N, Peters JA, Benson HE, *et al.* (2015a). The Concise Guide to PHARMACOLOGY 2015/16: G protein-coupled receptors. *Br J Pharmacol* **172**(24): 5744-5869.

Alexander SP, Fabbro D, Kelly E, Marrion N, Peters JA, Benson HE, *et al.* (2015b). The Concise Guide to PHARMACOLOGY 2015/16: Catalytic receptors. *Br J Pharmacol* **172**(24): 5979-6023.

Alexander SP, Fabbro D, Kelly E, Marrion N, Peters JA, Benson HE, *et al.* (2015c). The Concise Guide to PHARMACOLOGY 2015/16: Enzymes. *Br J Pharmacol* **172**(24): 6024-6109.

Alexander SP, Kelly E, Marrion N, Peters JA, Benson HE, Faccenda E, *et al.* (2015d). The Concise Guide to PHARMACOLOGY 2015/16: Overview. *Br J Pharmacol* **172**(24): 5729-5743.

Anas AA, Wiersinga WJ, de Vos AF, van der Poll T (2010). Recent insights into the pathogenesis of bacterial sepsis. *The Netherlands journal of medicine* **68**(4): 147-152.

Apaijai N, Pintana H, Chattipakorn SC, Chattipakorn N (2013). Effects of vildagliptin versus sitagliptin, on cardiac function, heart rate variability and mitochondrial function in obese insulin-resistant rats. *Br J Pharmacol* **169**(5): 1048-1057.

Arakawa M, Mita T, Azuma K, Ebato C, Goto H, Nomiyama T, *et al.* (2010). Inhibition of monocyte adhesion to endothelial cells and attenuation of atherosclerotic lesion by a glucagon-like peptide-1 receptor agonist, exendin-4. *Diabetes* **59**(4): 1030-1037.

Bataille D, Delagrangé P, Drucker DJ, Göke B, Hills R, Mayo KE, *et al.* (Last modified on 14/07/2015). Glucagon receptor family: GLP-1 receptor. *IUPHAR/BPS Guide to PHARMACOLOGY*

<http://guidetopharmacology.org/GRAC/ObjectDisplayForward?objectId=249>.

Cameron-Vendrig A, Reheman A, Siraj MA, Xu XR, Wang Y, Lei X, *et al.* (2016). Glucagon-like peptide-1 receptor activation attenuates platelet aggregation and thrombosis. *Diabetes*.

Chang SY, Kim DB, Ryu GR, Ko SH, Jeong IK, Ahn YB, *et al.* (2013). Exendin-4 inhibits iNOS expression at the protein level in LPS-stimulated Raw264.7 macrophage by the activation of cAMP/PKA pathway. *Journal of cellular biochemistry* **114**(4): 844-853.

Dai Y, Dai D, Wang X, Ding Z, Li C, Mehta JL (2014). GLP-1 agonists inhibit ox-LDL uptake in macrophages by activating protein kinase A. *Journal of cardiovascular pharmacology* **64**(1): 47-52.

Daiber A, August M, Baldus S, Wendt M, Oelze M, Sydow K, *et al.* (2004a). Measurement of NAD(P)H oxidase-derived superoxide with the luminol analogue L-012. *Free Radic Biol Med* **36**(1): 101-111.

Daiber A, Oelze M, Coldewey M, Bachschmid M, Wenzel P, Sydow K, *et al.* (2004b). Oxidative stress and mitochondrial aldehyde dehydrogenase activity: a comparison of pentaerythritol tetranitrate with other organic nitrates. *Mol Pharmacol* **66**(6): 1372-1382.

Elbrond B, Jakobsen G, Larsen S, Agerso H, Jensen LB, Rolan P, *et al.* (2002). Pharmacokinetics, pharmacodynamics, safety, and tolerability of a single-dose of NN2211, a long-acting glucagon-like peptide 1 derivative, in healthy male subjects. *Diabetes care* **25**(8): 1398-1404.

Graefe-Mody U, Rose P, Retlich S, Ring A, Waldhauser L, Cinca R, *et al.* (2012). Pharmacokinetics of linagliptin in subjects with hepatic impairment. *British journal of clinical pharmacology* **74**(1): 75-85.

Gromada J, Ding WG, Barg S, Renstrom E, Rorsman P (1997). Multisite regulation of insulin secretion by cAMP-increasing agonists: evidence that glucagon-like peptide 1 and glucagon act via distinct receptors. *Pflugers Archiv : European journal of physiology* **434**(5): 515-524.

Gryglewski RJ, Szczeklik A, Wandzilak M (1987). The effect of six prostaglandins, prostacyclin and iloprost on generation of superoxide anions by human polymorphonuclear leukocytes stimulated by zymosan or formyl-methionyl-leucyl-phenylalanine. *Biochem Pharmacol* **36**(24): 4209-4213.

Gupta AK, Verma AK, Kailashiya J, Singh SK, Kumar N (2012). Sitagliptin: anti-platelet effect in diabetes and healthy volunteers. *Platelets* **23**(8): 565-570.

Hausding M, Jurk K, Daub S, Kroller-Schon S, Stein J, Schwenk M, *et al.* (2013). CD40L contributes to angiotensin II-induced pro-thrombotic state, vascular inflammation, oxidative stress and endothelial dysfunction. *Basic Res Cardiol* **108**(6): 386.

Iba T, Nakarai E, Takayama T, Nakajima K, Sasaoka T, Ohno Y (2009). Combination effect of antithrombin and recombinant human soluble thrombomodulin in a lipopolysaccharide induced rat sepsis model. *Critical care* **13**(6): R203.

Jurk K, Lahav J, H VANA, Brodde MF, Nofer JR, Kehrel BE (2011). Extracellular protein disulfide isomerase regulates feedback activation of platelet thrombin generation via modulation of coagulation factor binding. *Journal of thrombosis and haemostasis : JTH* **9**(11): 2278-2290.

Kameoka J, Tanaka T, Nojima Y, Schlossman SF, Morimoto C (1993). Direct association of adenosine deaminase with a T cell activation antigen, CD26. *Science* **261**(5120): 466-469.

Kroller-Schon S, Knorr M, Hausding M, Oelze M, Schuff A, Schell R, *et al.* (2012). Glucose-independent improvement of vascular dysfunction in experimental sepsis by dipeptidyl-peptidase 4 inhibition. *Cardiovasc Res* **96**(1): 140-149.

Kroller-Schon S, Steven S, Kossmann S, Scholz A, Daub S, Oelze M, *et al.* (2014). Molecular mechanisms of the crosstalk between mitochondria and NADPH oxidase through reactive oxygen species-studies in white blood cells and in animal models. *Antioxid Redox Signal* **20**(2): 247-266.

Ku HC, Chen WP, Su MJ (2010). GLP-1 signaling preserves cardiac function in endotoxemic Fischer 344 and DPP4-deficient rats. *Naunyn-Schmiedeberg's archives of pharmacology* **382**(5-6): 463-474.

Levi M, Ten Cate H (1999). Disseminated intravascular coagulation. *The New England journal of medicine* **341**(8): 586-592.

Levi M, van der Poll T (2010). Inflammation and coagulation. *Critical care medicine* **38**(2 Suppl): S26-34.

Levy MM, Artigas A, Phillips GS, Rhodes A, Beale R, Osborn T, *et al.* (2012). Outcomes of the Surviving Sepsis Campaign in intensive care units in the USA and Europe: a prospective cohort study. *The Lancet. Infectious diseases* **12**(12): 919-924.

Marguet D, Baggio L, Kobayashi T, Bernard AM, Pierres M, Nielsen PF, *et al.* (2000). Enhanced insulin secretion and improved glucose tolerance in mice lacking CD26. *Proc Natl Acad Sci U S A* **97**(12): 6874-6879.

Martin M, Huguet J, Centelles JJ, Franco R (1995). Expression of ecto-adenosine deaminase and CD26 in human T cells triggered by the TCR-CD3 complex. Possible role of adenosine deaminase as costimulatory molecule. *Journal of immunology* **155**(10): 4630-4643.

Matsubara J, Sugiyama S, Sugamura K, Nakamura T, Fujiwara Y, Akiyama E, *et al.* (2012). A dipeptidyl peptidase-4 inhibitor, des-fluoro-sitagliptin, improves endothelial function and

reduces atherosclerotic lesion formation in apolipoprotein E-deficient mice. *J Am Coll Cardiol* **59**(3): 265-276.

Moritoh Y, Takeuchi K, Asakawa T, Kataoka O, Odaka H (2009). Combining a dipeptidyl peptidase-4 inhibitor, alogliptin, with pioglitazone improves glycaemic control, lipid profiles and beta-cell function in db/db mice. *Br J Pharmacol* **157**(3): 415-426.

Oelze M, Warnholtz A, Faulhaber J, Wenzel P, Kleschyov AL, Coldewey M, *et al.* (2006). NADPH oxidase accounts for enhanced superoxide production and impaired endothelium-dependent smooth muscle relaxation in BKbeta1^{-/-} mice. *Arterioscler Thromb Vasc Biol* **26**(8): 1753-1759.

Pabreja K, Mohd MA, Koole C, Wootten D, Furness SG (2014). Molecular mechanisms underlying physiological and receptor pleiotropic effects mediated by GLP-1R activation. *Br J Pharmacol* **171**(5): 1114-1128.

Pawson AJ, Sharman JL, Benson HE, Faccenda E, Alexander SP, Buneman OP, *et al.* (2014). The IUPHAR/BPS Guide to PHARMACOLOGY: an expert-driven knowledgebase of drug targets and their ligands. *Nucleic acids research* **42**(Database issue): D1098-1106.

Plum A, Jensen LB, Kristensen JB (2013). In vitro protein binding of liraglutide in human plasma determined by reiterated stepwise equilibrium dialysis. *Journal of pharmaceutical sciences* **102**(8): 2882-2888.

Schafer A, Burkhardt M, Vollkommer T, Bauersachs J, Munzel T, Walter U, *et al.* (2003). Endothelium-dependent and -independent relaxation and VASP serines 157/239 phosphorylation by cyclic nucleotide-elevating vasodilators in rat aorta. *Biochemical pharmacology* **65**(3): 397-405.

Schouten M, Wiersinga WJ, Levi M, van der Poll T (2008). Inflammation, endothelium, and coagulation in sepsis. *Journal of leukocyte biology* **83**(3): 536-545.

Scrocchi LA, Brown TJ, MaClusky N, Brubaker PL, Auerbach AB, Joyner AL, *et al.* (1996). Glucose intolerance but normal satiety in mice with a null mutation in the glucagon-like peptide 1 receptor gene. *Nature medicine* **2**(11): 1254-1258.

Shah Z, Kampfrath T, Deiuliis JA, Zhong J, Pineda C, Ying Z, *et al.* (2011). Long-term dipeptidyl-peptidase 4 inhibition reduces atherosclerosis and inflammation via effects on monocyte recruitment and chemotaxis. *Circulation* **124**(21): 2338-2349.

Simpson PJ, Mickelson J, Fantone JC, Gallagher KP, Lucchesi BR (1987). Iloprost inhibits neutrophil function in vitro and in vivo and limits experimental infarct size in canine heart. *Circulation research* **60**(5): 666-673.

Steven S, Hausding M, Kroller-Schon S, Mader M, Mikhed Y, Stamm P, *et al.* (2015a). Gliptin and GLP-1 analog treatment improves survival and vascular inflammation/dysfunction in animals with lipopolysaccharide-induced endotoxemia. *Basic Res Cardiol* **110**(2): 6.

Steven S, Munzel T, Daiber A (2015b). Exploiting the Pleiotropic Antioxidant Effects of Established Drugs in Cardiovascular Disease. *International journal of molecular sciences* **16**(8): 18185-18223.

Sturis J, Gotfredsen CF, Romer J, Rolin B, Ribel U, Brand CL, *et al.* (2003). GLP-1 derivative liraglutide in rats with beta-cell deficiencies: influence of metabolic state on beta-cell mass dynamics. *Br J Pharmacol* **140**(1): 123-132.

Tchaikovski SN, BJ VANV, Rosing J, Tans G (2007). Development of a calibrated automated thrombography based thrombin generation test in mouse plasma. *Journal of thrombosis and haemostasis : JTH* **5**(10): 2079-2086.

Tokalov SV, Bachiller D (2012). IV delivery of fluorescent beads. *Chest* **141**(3): 833-834; author reply 834-835.

Wang Z, Wang RM, Owji AA, Smith DM, Ghatei MA, Bloom SR (1995). Glucagon-like peptide-1 is a physiological incretin in rat. *The Journal of clinical investigation* **95**(1): 417-421.

Zhong J, Rao X, Rajagopalan S (2013). An emerging role of dipeptidyl peptidase 4 (DPP4) beyond glucose control: potential implications in cardiovascular disease. *Atherosclerosis* **226**(2): 305-314.

Ziegler-Heitbrock HW, Thiel E, Futterer A, Herzog V, Wirtz A, Riethmuller G (1988). Establishment of a human cell line (Mono Mac 6) with characteristics of mature monocytes. *International journal of cancer. Journal international du cancer* **41**(3): 456-461.

Accepted

Legends to figures

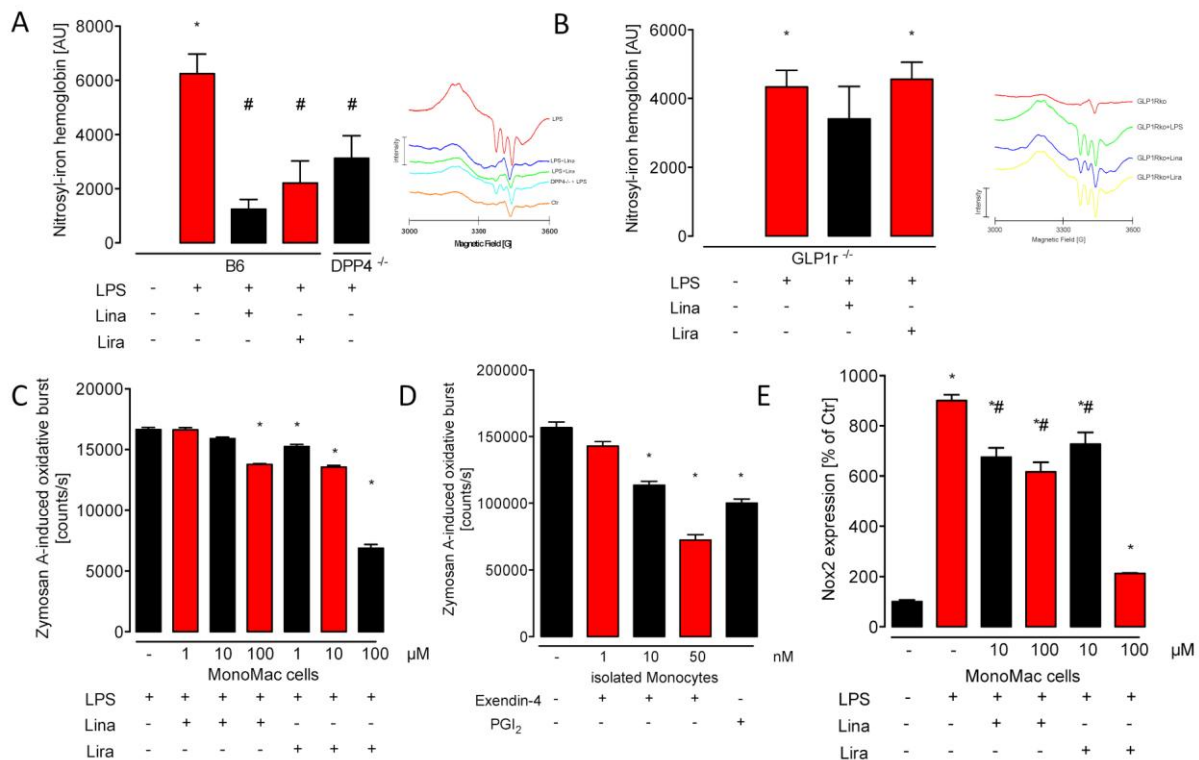


Figure 1

GLP-1 receptor signalling reduces iNOS dependent NO formation and mRNA expression in vivo and inhibits oxidative burst in monocytes. **(A,B)** Whole blood Hb-NO levels were determined by electron paramagnetic resonance spectroscopy as a read-out of iNOS activity. NADPH oxidase activity in **(C)** cultured and **(D)** isolated (from human whole blood) monocytes was determined by chemiluminescence (L-012) after zymosan-A stimulation. **(E)** qRT-PCR was used to determine mRNA expression levels of Nox2 in cultured monocytes. The data are mean \pm SEM from 6-18 **(A,B)**, cells from at least 8 different cell culturing wells **(C,D)** or at least 3 different individuals **(E)** were used. **(A)** *, $p < 0.05$ vs. B6 and #, $p < 0.05$ vs. B6+LPS; **(B)** *, $p < 0.05$ vs. GLP-1r^{-/-}; **(C-E)** *, $p < 0.05$ vs. control and #, $p < 0.05$ vs. +LPS.

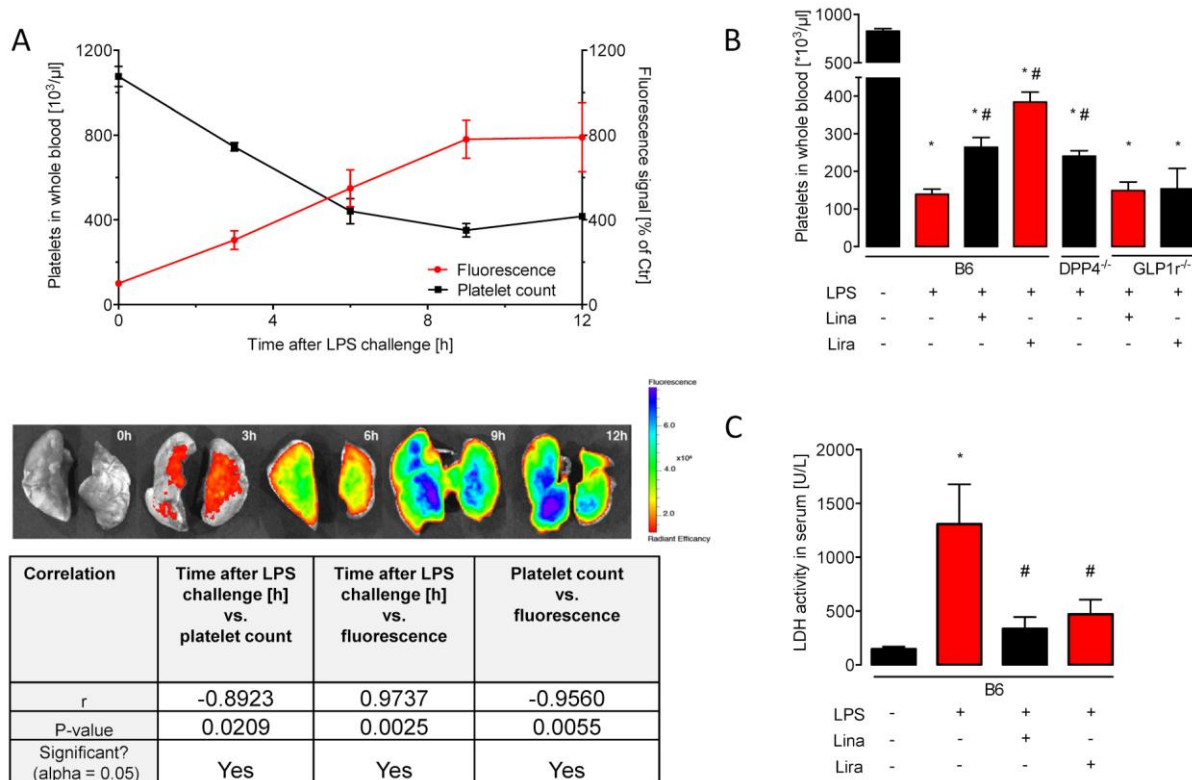


Figure 2

Time-course/correlation of thrombocytopenia and fluorescence bead imaging as marker for pulmonary microvascular thrombosis – GLP-1 receptor signalling improves thrombocytopenia and LDH-activity in endotoxaemia. **(A)** Platelet count in whole blood and fluorescence signals in lungs of wild-type mice were measured over a 12 h time-course after LPS-injection. The fluorescence signal was determined after injection of fluorescent beads by using fluorescence imaging. Representative images of lungs are shown below. **(B)** Platelet count in endotoxaemic wild-type, DPP-4^{-/-} and GLP-1r^{-/-} mice was determined 24 hours after LPS-injection. **(C)** Lactate dehydrogenase (LDH) activity was measured in serum 24 hours after LPS-injection. The data are mean \pm SEM from **(A)** 3 mice per time point, **(B)** 6-21, **(C)** 3-5 mice per/group. *, $p < 0.05$ vs. B6 and #, $p < 0.05$ vs. B6+LPS.

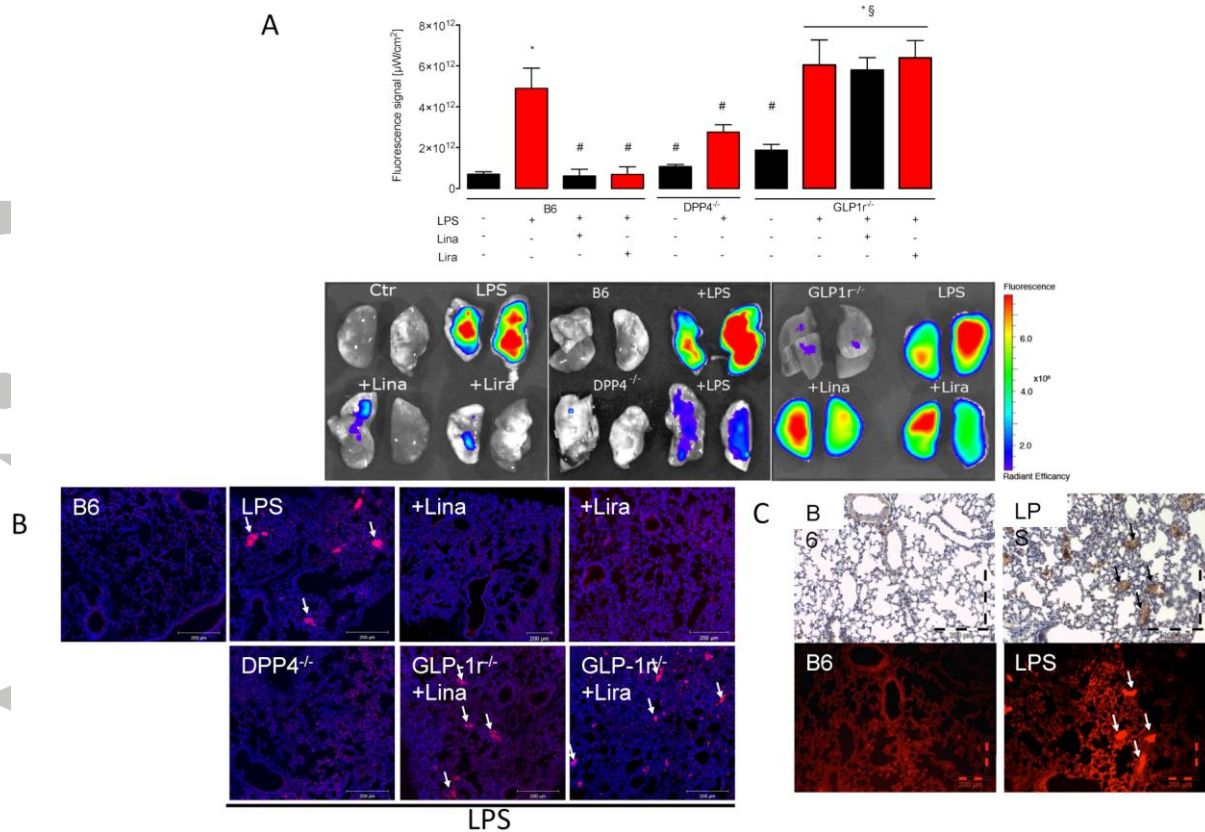


Figure 3

GLP-1 receptor signalling improves microvascular thrombosis in endotoxaemia. **(A)** Microvascular thrombosis was detected by fluorescence imaging using fluorescent micro beads in endotoxaemic wild-type mice, DPP-4^{-/-} mice and GLP1r^{-/-} mice. Representative images of lungs are shown below. **(B)** Microvascular thrombosis was further detected by fluorescence microscopy of paraffin embedded lung sections. Nuclei are DAPI stained (blue) and pre-injected fluorescence beads (red) were excited at their specific wavelength. **(C)** Fluorescence beads and fibrinogen deposit were co-localized in lung sections by a specific antibody staining and excitation of fluorescence beads at their specific wavelength. **(B,C)** Representative sections selected from at least 4 animals per group are shown. The data are mean \pm SEM from **(A-C)** 4-6 mice/group. *, $p < 0.05$ vs. B6; #, $p < 0.05$ vs. B6+LPS; § $p < 0.05$ vs. GLP-1r^{-/-}.

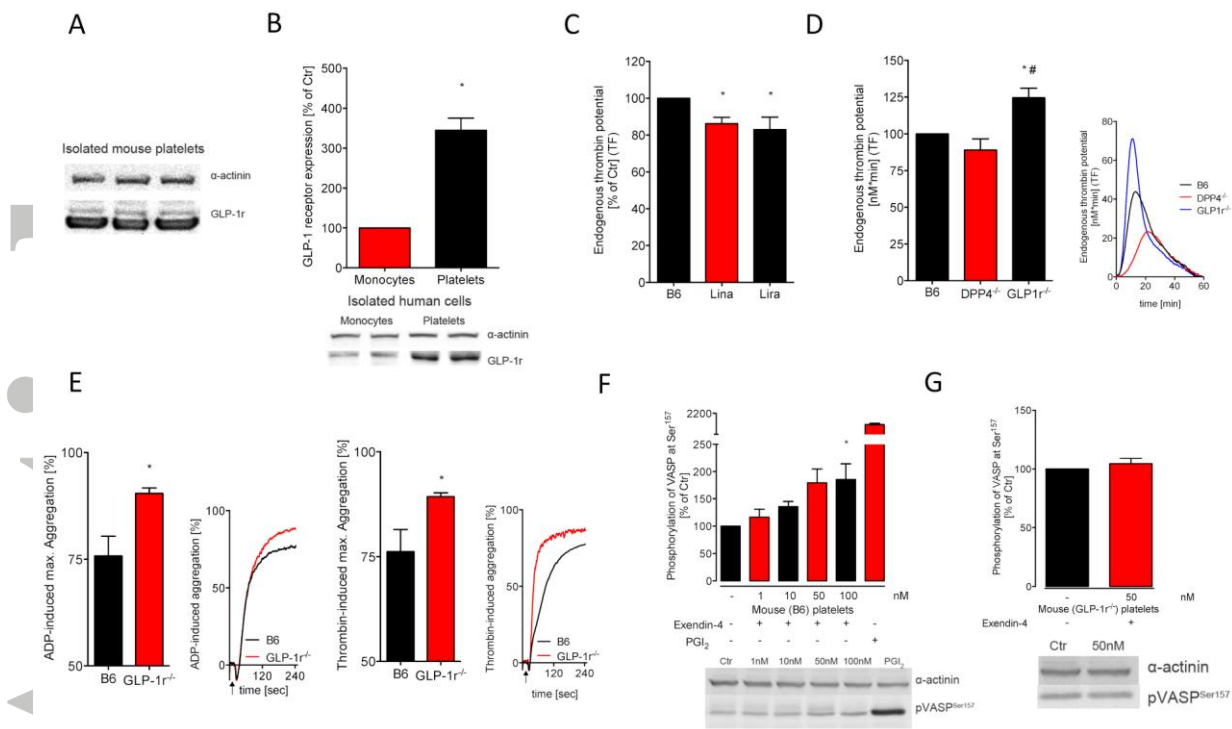


Figure 4

GLP-1 receptor signalling reduces murine platelet reactivity cAMP/PKA-dependently. **(A)** GLP-1 receptor protein was detected by Western blot in platelets isolated from wild-type mouse and in **(B)** platelets and monocytes isolated from human whole blood. **(C,D)** Tissue factor-dependent thrombin generation was measured by calibrated automated thrombography (CAT) assay in platelet-rich plasma of mice. Representative thrombography curves are shown. **(E)** Thrombin/ADP-induced platelet aggregation was measured in platelet-rich plasma of mice. Representative aggregation curves are shown. Arrow indicates time-point of thrombin/ADP-addition. **(F)** cAMP-dependent phosphorylation of VASP at Ser¹⁵⁷ in isolated wild-type or **(G)** GLP-1r^{-/-} mouse platelets was detected by Western blot using a specific antibody. Prostacyclin (PGI₂) was used at a concentration of 0.2 ng/ml. The data are mean \pm SEM from **(A)** 3 animals/group **(B)** 4 human individuals **(C,D)** 6-11, **(E)** 3 and **(F,G)** 4-6 animals/group **(B)** *, $p < 0.05$ vs. Monocytes **(C,D)** *, $p < 0.05$ vs. B6, #, $p < 0.05$ vs. DPP-4^{-/-}. **(E-G)** *, $p < 0.05$ vs. Ctr.

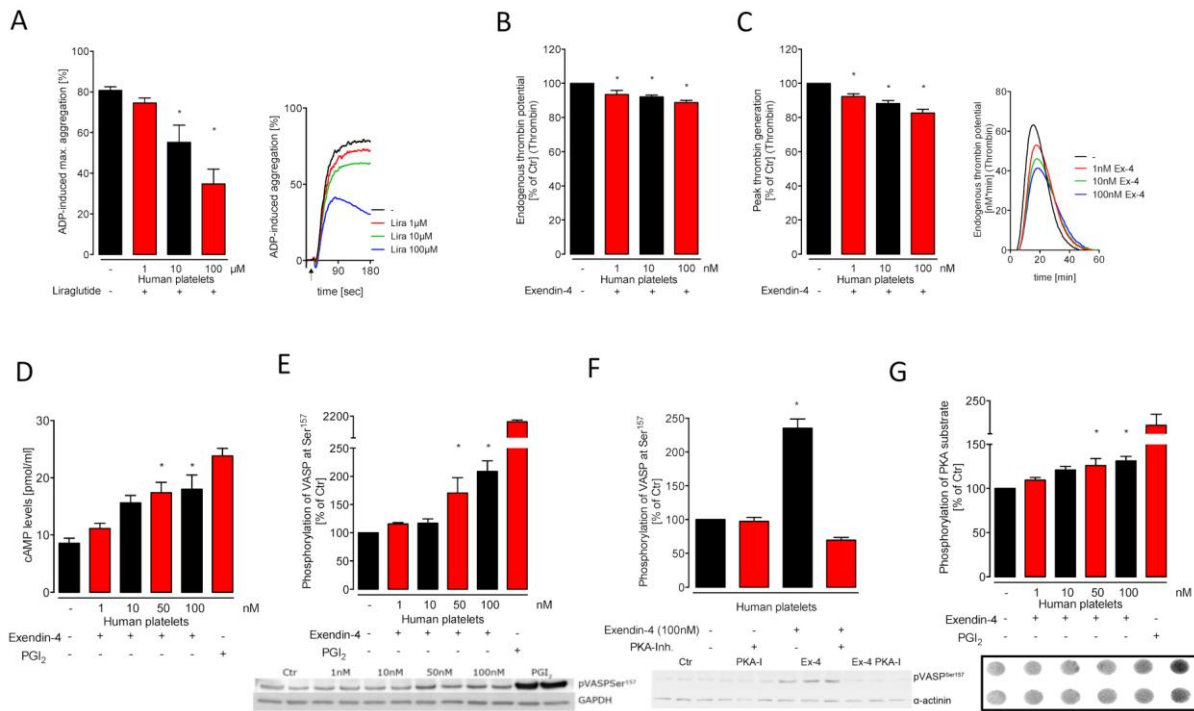


Figure 5

GLP-1 receptor signalling reduces human platelet reactivity cAMP/PKA-dependently. **(A)** ADP-induced platelet aggregation was measured in human platelet-rich plasma after liraglutide ex vivo incubation. Representative aggregation curves are shown. Arrow indicates time-point of ADP addition. **(B,C)** Thrombin-dependent thrombin generation (endogenous thrombin potential and peak thrombin generation) was measured by calibrated automated thrombography (CAT) assay in platelet-rich plasma of human after exendin-4 ex vivo incubation. Representative thrombography curves are shown. **(D)** cAMP levels in isolated human platelet was determined by a commercial ELISA. **(E)** cAMP-dependent phosphorylation of VASP at Ser¹⁵⁷ in isolated human platelets was detected by Western blot using a specific antibody, **(F)** which was blocked by a PKA-inhibitor (1 μM). **(G)** Phospho^{Ser/Thr} PKA substrate was examined by dot blot using a specific antibody. Prostacyclin (PGI₂) was used at a concentration of 0.2 ng/ml. The data are mean ± SEM from **(A-F)** 4-6 different individuals per group. **(A-G)** *, p<0.05 vs. Ctr.

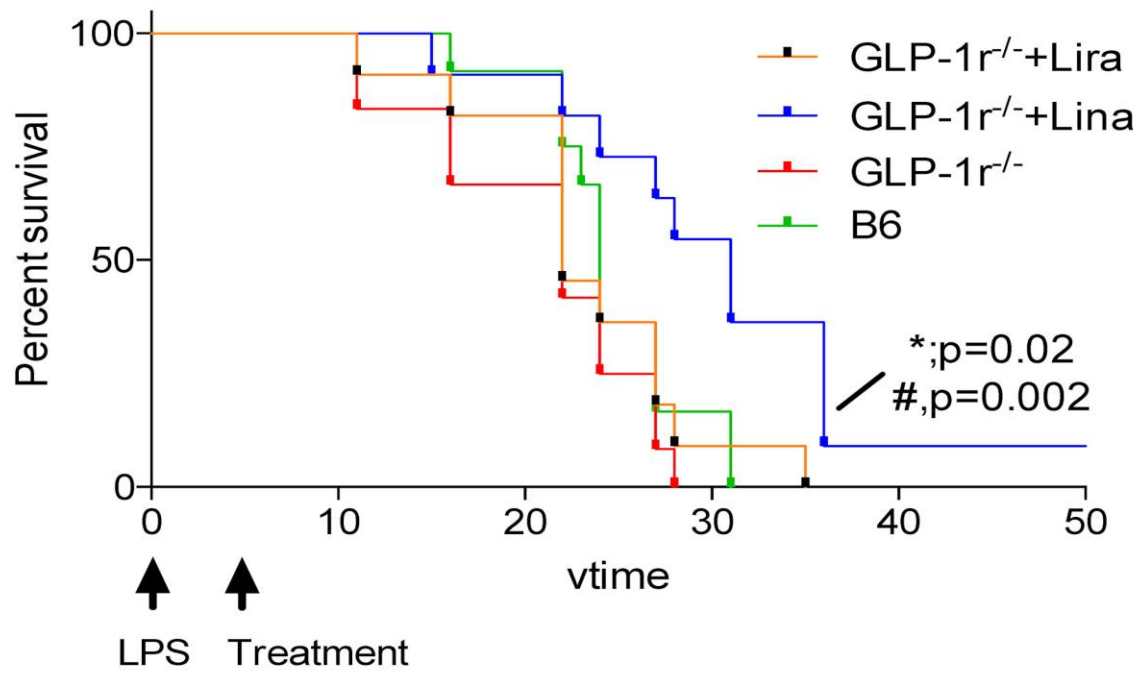


Figure 6

Effect of DPP-4 inhibition (linagliptin, Lina) and GLP-1 analogue (liraglutide, Lira) supplementation on survival of endotoxaemic GLP-1^{r-/-} and wild type (B6) mice. Mortality of endotoxaemic mice was assessed by Kaplan-Meier curves recording the survival in dependence of time. 17.5 mg/kg LPS or solvent were administered by i.p. injection. DPP-4 inhibitor (Lina: 5 mg/kg/d s.c. for 3 d) and GLP-1 analogue (Lira: 200 µg/kg/d s.c. for 3 d) treatment was started 6 h after induction of endotoxaemia. A total number of 48 animals and 12 animals per group were used (*, p=0.02 vs. B6 group, #, p<0.002 vs. GLP-1^{r-/-} group).

Supporting information

Additional Supporting Information may be found in the online version of this article at the publisher's web-site:

Figure S1 (A) Dipeptidyl peptidase-4 activity was detected using a specific peptide substrate with a terminal coumarin derivative (H-Ala-Pro-7-amido-4-trifluoromethylcoumarin; Bachem, Bubendorf, Switzerland; final concentration in the assay, 100 μ M) allowing quantification in a fluorescence microplate reader upon cleavage by DPP-4. These analyses were performed at the Department of Cardio Metabolic Diseases Research, Boehringer Ingelheim Pharma GmbH and Co. KG. **(B)** Expression of GLP-1 receptor was quantified by qRT-PCR. The data are mean \pm SEM from 8 mice/group. *, $p < 0.05$ vs. B6.

Figure S2 (A-D) qRT-PCR was used to determine mRNA expression levels of iNOS, P-selectin, vascular adhesion molecule-1 (VCAM-1) and interleukin-6 (IL-6) in aortic tissue. Aortic tissue of 4 mice/group **(A-D)** *, $p < 0.05$ vs. B6 and #, $p < 0.05$ vs. B6+LPS.

Figure S3 (A) ADP- and **(B)** thrombin-induced platelet aggregation was measured in platelet-rich plasma of human subjects. Effects of exendin-4 **(A)** and liraglutide **(B)** are shown. Representative aggregation curves are shown for liraglutide experiments. **(C, D)** Effects of liraglutide on thrombin-dependent thrombin generation was measured by calibrated automated thrombography (CAT) assay in platelet-rich plasma of human subjects. The data are mean \pm SEM from 3-4 human samples. *, $p < 0.05$ vs. untreated sample.

Figure S4 (A-C) Endothelium-dependent (ACh) relaxation was determined by isometric tension studies in mouse aortic ring segments. In order to provide best overview to the reader same curves for B6 and B6+LPS are presented in different figures (dashed lines). Panel **C**: green and purple groups were also treated with LPS. A total number of 12-37 aortic rings from at least 6 animals/group **(A-C)** was used. **(A,B)** *, $p < 0.05$ vs. B6 and #, $p < 0.05$ vs. B6+LPS. **(C)** *, $p < 0.05$ vs. GLP-1 $r^{-/-}$ and #, $p < 0.05$ vs. GLP-1 $r^{-/-}$ +LPS.